HHS Public Access

Author manuscript

J Bone Miner Res. Author manuscript; available in PMC 2018 July 01.

Published in final edited form as:

J Bone Miner Res. 2017 July ; 32(7): 1442–1454. doi:10.1002/jbmr.3133.

Skeletal colonization by breast cancer cells is stimulated by an osteoblast and β2AR-dependent neo-angiogenic switch

Patrick L. Mulcrone, B.A.[1,5], **J. Preston Campbell, PhD**[1], **Lise Clément-Demange, PhD**[8], **Ana Lia Anbinder, PhD**[4], **Alyssa R. Merkel, M.S.**[2,3,5], **Rolf A. Brekken, PhD**[6], **Julie A. Sterling, PhD**[1,2,3,5], and **Florent Elefteriou, PhD**[3,7,8]

[1]Department of Cancer Biology, Vanderbilt University, Nashville, TN, USA

[2]Department of Veterans Affairs, Tennessee Valley Healthcare System, Nashville, TN, USA

[3]Department of Medicine, Division of Clinical Pharmacology, Vanderbilt University Nashville, TN, USA

[4]Department of Biosciences and Oral Diagnosis, São José dos Campos School of Dentistry, Univ. Estadual Paulista-UNESP, São José dos Campos, Brazil

[5]Vanderbilt Center for Bone Biology, Vanderbilt University, Nashville, TN, USA

[6]Department of Surgery and Hamon Center for Therapeutic Oncology Research, UT Southwestern, Dallas, TX, USA

[7]Department of Molecular and Human Genetics, Baylor College of Medicine, Houston, TX, USA

[8]Department of Orthopedic Surgery, Baylor College of Medicine, Houston, TX, USA

Abstract

The skeleton is a common site for breast cancer metastasis. Although significant progress has been made to manage osteolytic bone lesions, the mechanisms driving the early steps of the bone metastatic process are still not sufficiently understood to design efficacious strategies needed to inhibit this process and offer preventative therapeutic options. Progression and recurrence of breast cancer, as well as reduced survival of patients with breast cancer, are associated with chronic stress, a condition known to stimulate sympathetic nerve outflow. In this study, we show that stimulation of the beta 2-adrenergic receptor (β2AR) by isoproterenol, used as a pharmacological surrogate of sympathetic nerve activation, led to increased blood vessel density and *Vegf-a* expression in bone. It also raised levels of secreted Vegf-a in osteoblast cultures, and accordingly, the conditioned media from isoproterenol-treated osteoblast cultures promoted new vessel formation in two *ex vivo* models of angiogenesis. Blocking the interaction between Vegf-a and its receptor, Vegfr2, blunted the increase in vessel density induced by isoproterenol. Genetic loss of the β2AR globally, or specifically in type 1 collagen-expressing osteoblasts, diminished the increase in Vegf-positive osteoblast number and bone vessel density induced by isoproterenol, and

Authors' roles: Study design: PLM, JPC, ALA, RAB, JAS, FE. Study conduct, data analysis and collection: PLM, JPC, LCD, ALA, ARM, FE. Data interpretation: PLM, JPC, ARM, RAB, JAS, FE. Drafting and revising manuscript: PLM, JPC, ARM, JAS, FE. Approval of final version of manuscript: PLM, JAS, FE.

Disclosures

All authors have no conflicts of interest to disclose.

reduced the higher incidence of bone metastatic lesions induced by isoproterenol following intracardiac injection of an osteotropic variant of MDA-MB-231 breast cancer cells. Inhibition of the interaction between Vegf-a and Vegfr2 with the blocking antibody mcr84 also prevented the increase in bone vascular density and bone metastasis triggered by isoproterenol. Together, these results indicate that stimulation of the β2AR in osteoblasts triggers a Vegf-dependent neo-angiogenic switch that promotes bone vascular density and the colonization of the bone microenvironment by metastatic breast cancer cells.

According to the American Cancer Society, ~250,000 US women are diagnosed with breast cancer each year, and around 41,000 will ultimately succumb to the disease (1). Up to 75% of breast cancer patients with diffuse metastatic disease will develop a bone lesion (2). Bony metastases lead to hypercalcemia, intractable bone pain, bone destruction, and fracture. Although treatments are now available to limit bone destruction when skeletal metastases are detected, the clinical management of breast cancer patients remains palliative, and life expectancy is still limited (2). Uncovering the major determinants controlling the nesting of metastatic cancer cells within the skeleton, at early stage of the disease, is necessary to design new strategies to treat bone metastases and prevent the complications associated with these lesions.

Clues about the conditions driving the osteotropism of metastatic cancer cells can be obtained from retrospective studies, in which factors associated with reduced survival are identified. In that regard, chronic emotional stress has been linked to higher breast cancer recurrence, reduced survival, and poor prognosis (3–10), and β-blockers were associated with prolonged survival in breast cancer patients when treatment was initiated at time of diagnosis (9–10). A common factor between these studies is the activity of the sympathetic nervous system (SNS) that is stimulated by chronic psychosocial stress and whose action is antagonized by β-blockers.

The skeleton is richly vascularized, with arterial vessels dividing within the marrow into arterioles and capillaries that span throughout the bone marrow and supply sinusoids. An interesting observation is that this vascular network is closely associated with nerves, including dopamine β-hydroxylase-positive sympathetic fibers that have a circumferential perivascular distribution in bone but also branching varicosities in proximity with bone trabeculae (11). Previous studies also provided evidence that sympathetic outflow increases vascular endothelial growth factor (VEGF) levels and vascular density in primary tumors (10,12). While these studies focused on the effect of sympathetic nerves in tumors, the same scrutiny has not been given to the different microenvironments to which breast cancer cells spread.

Severe emotional stress stimulates the Hypothalamic-Pituitary Axis (HPA) and sympathetic outflow, causing the release of peripheral catecholamines that stimulate post-synaptic β-adrenergic receptors (βARs). Osteoblasts mainly express the β2AR (13–15) and respond to βAR agonists by an increase in Receptor Activator of Nf-κB ligand (RANKL), a key cytokine involved in the maturation of osteoclasts and bone turnover (16). Our group and others have shown that high sympathetic outflow and HPA activation triggered by chronic immobilization stress promotes breast cancer homing to lungs and bone, implicating

macrophages and RANK/RANKL signaling, respectively (6,17). Daily administration with the non-selective β1/β2AR agonist, isoproterenol (ISO), triggered the same effects, validating this approach to mimic an increase in sympathetic nerve outflow without overt effect on the HPA axis. However, a retrospective study by Santini *et al.* showed that a large proportion of bone lesions in breast cancer patients contained RANK-negative cells, suggesting that additional mechanisms might be at play for sympathetic nerves signals to influence the homing of metastatic cancer cells into the skeleton (18).

In this study, we show that βAR stimulation in mice promotes the expansion of the post-natal bone vascular network via an osteoblastic βAR- and VEGF-dependent mechanism, and that this stromal, neo-angiogenic switch contributes to the colonization of the bone marrow environment by breast cancer cells.

Methods

In Vivo Drug Treatments

The Institutional Animal Care and Use Committee at Vanderbilt University Medical Center approved all procedures. All mice used for *in vivo* studies were female. Mice were housed 2–5 per cage, and any mice on the Rag2−/− background were housed in sterile cages, also 2–5 per cage. The β-agonist Isoproterenol (ISO, Sigma #I6504-1G) was injected intraperitoneally each day for 3–6 weeks at a dose of 3mg/kg in 100 μL of sterile PBS. For both the tumor and vessel characterization studies, 200 μg mcr84 (kindly shared by Dr. Brekken) or control IgG2 antibodies (generated by the Vanderbilt University Antibody and Protein Core) were injected intraperitoneally twice a week for 6 weeks. The mcr84 antibody is a mouse chimeric IgG2, monoclonal antibody that targets VEGF-A specifically and prevents it from binding to VEGFR2 (19, 20).

Generation of Rag2−/−; Adrβ2$^{flox/flox}$; Col1-Cre Mice

β2AR$_{ob}$KO mice (*Adrβ2*$^{flox/flox}$; *mouse 2.3kb Col1-cre* on the C57BL/6 background) were generated by crossing the mouse 2.3kb *α1*(1)-*collagen-cre* transgenic line (21) with the *Adrβ2*$^{flox/flox}$ mutant mouse line expressing a floxed allele of *Adrβ2* (22), kindly shared by Dr. Karsenty. For tumor studies utilizing human MDA-MB-231 cells, β2AR$_{ob}$KO mice were bred with immunodeficient *Rag2−/−* mice to allow human-derived tumor take in the resulting double KO mice. *Rag2*−/−; *Adrβ2*$^{flox/flox}$; *2.3kbCol1-cre*-positive mice are herein called *Rag/β2AR$_{ob}$KO*, and control littermates (*Rag2*−/−; *Adrβ2*$^{flox/flox}$, *2.3kbCol1-cre*-negative mice) are herein called *Rag/WT*. These immune-compromised mice have experimental advantages and limitations. They allow the use of human cancer cells in a genetically-modified murine host and exclude the potential contribution of βAR-expressing immune cells when interpreting results, thus reducing the complexity of the experimental system. However, the age of these mice and their immune-compromised status is not clinically relevant, hence the relevance of these findings will need to be further addressed in immune-competent models and in humans.

Intracardiac Injection of Cancer Cells

For all experiments requiring tumor cells, a bone metastatic clonal variant of the human triple negative breast cancer cell line MDA-MB-231 was used (23). This variant was established by serial *in vivo* passage of parental MDA-MB-231 cells (ATCC) that metastasized to bone following intracardiac injection. These osteotropic MDA-MB-231 cells were cultured in 10% DMEM (Gibco) containing 10% fetal bovine serum and 1% penicillin/streptomycin, trypsinized at 70% confluence, and re-suspended in cold PBS at 10^6 cells/ml. Six-week old, *Rag/WT* or *Rag/β2AR$_{ob}$KO* female mice were anesthetized with isoflurane and injected in the left cardiac ventricle with 100 μL of cell suspension (a total of 10^5 cells) as previously described (7).

Imaging Analysis

Bone metastases were assessed via a Faxitron digital x-ray imaging system. Osteolytic lesions were quantified in the hind limbs and the forelimbs at end point (28 days) from Faxitron images by ROI analysis using MetaMorph software (Molecular Devices, Inc.). Measurements were performed blinded from treatment/genotype and by three persons. Presence of bone tumors was confirmed by histology. Lesion number was calculated as total number of hind limb and forelimb osteotropic lesions per mouse. Lesion area was analyzed from the hind limb and forelimb lesions present by x-ray and calculated by pixel area using the MetaMorph Software.

Histomorphometry

For histological analyses, hind limbs were dissected and immediately placed into neutral buffered formalin for 48 hours at 4°C on a plate shaker. The bones were then transferred to 20% EDTA for 5 days at 4°C for decalcification. Following this step, the bones were processed for paraffin sectioning according to standard protocols. Samples were mounted in wax blocks and sectioned at 6 μm. Sections were stained for Vegf- a, endomucin, or CD31 according to the manufacturers' instructions (Primary- Abcam #46154 (5μg/mL), Santa Cruz sc-65495 (1:100) or Abcam #56299 (1:100); Secondary- Santa Cruz sc-2005 (1:500)). A 20 μg/mL proteinase K solution (Roche #03115828001) was applied for 20 minutes to sections for antigen retrieval. Signal was detected by immunohistochemistry using the NOVA Red Kit (Vector Laboratories, #SK-4800) or immunofluorescence (Primary- Santa Cruz sc-65495 (1:100); Secondary- Thermo Fisher Alex Fluor 647 A-21247(1:500) (24). Osteoclast and osteoblast number and size were assessed using the Osteomeasure imaging software (OsteoMetrics, Decatur, GA). Hind limb sections were analyzed for osteoclasts by counting tartrate resistant acid phosphatase (TRAP)-positive cells with 3 or more nuclei along the bone surface. Sections were counterstained with hematoxylin. Osteoblasts were counted based on morphology, contact with bone tissue, and a series of at least 3 similar cells. Immunohistochemistry images were captured using an Olympus BX41 Microscope, and immunofluorescence results were analyzed using a laser-scanning microscope (510/Meta/FCS Carl Zeiss, Inc.) with 10× and 20× objectives using 0.7× zoom.

Mouse Metatarsal Assay

Two day-old C57BL/6 pups were sacrificed, and their hind limb metatarsals were dissected as previously described (25). Metatarsals were cultured in α-MEM medium (Gibco) containing 10% fetal bovine serum (hereby 10% α-MEM) and 1% penicillin/streptomycin in a 24-well plate for 14 days. For conditioned media (CM), MC3T3 mouse osteoblasts were cultured in 10% α-MEM and passaged in a 1:3 ratio. Once cells became 70% confluent, cells were treated with PBS or drug overnight (18 hours) in 10% α-MEM. The following morning, CM was collected. After 3 days in 10% α-MEM, metatarsals were treated with one of the following: unconditioned 10% α-MEM or the CM of PBS, 10 μM norepinephrine (NE), or 10 μM isoproterenol (ISO)-treated osteoblasts. After 4 CM treatments over the 2-week experimental time course, metatarsals were fixed with 10% Zinc formalin and stained for CD31 (Primary- BD Pharmingen #553370 (1:100), Secondary- Santa Cruz sc-2005 (1:500)). The number of vessels sprouting from the bones was calculated. Measurements were performed blinded from treatment by three persons.

Primary Mouse Bone Marrow Stromal Cell and Mouse Bone Marrow Endothelial Cell Cultures

Hind limbs from WT C57BL/6 mice were used to prepare primary mouse bone marrow stromal cells (BMSCs). Femur and tibia were stripped of skin and muscles, distal and proximal epiphyses were cut off, and each bone was inserted into a punctured 0.5mL tube placed into a 1.5mL tube containing 1mL of 10% α-MEM. Tubes were centrifuged for 2 mins at 13.2×1000 rpm at 4°C. Resulting pellets were resuspended in 10% α-MEM, and cells were plated. Cultures were grown in 10% α-MEM for 4 days, and then switched to an osteogenic medium (10% α-MEM containing 50ug/mL ascorbic acid (Sigma, #A-5950) and 5 mM beta-glycerophosphate (Sigma, #G9891-25G)) for 8–14 days.

Primary mouse bone marrow endothelial cells (BMEC) were harvested as previously described (26). Mouse hind limb bone marrow was flushed and centrifuged in Complete Endothelial Cell Growth Media (ScienCell #1001). Cells were plated on tissue culture dishes or in tissue culture flasks coated with 4 μg/mL fibronectin (Gibco #33016015) in Complete Endothelial Cell Growth Media. After 7 days, cells were used for experiments.

Tube Formation Assay

Twenty-four well plates were coated with 200 μL of growth factor reduced matrigel (Corning #354230) for 45 mins. at 37°C before 30,000 HUVECs (Gibco #C0035C), or BMECs from wild-type C57BL/6 mice were plated and cultured in 500 μL of Basal Endothelial Cell Growth Media (ScienCell #1001). Cells were then treated with human (10ng/mL) or mouse (50ng/mL) rVEGF (R&D Biosystems #293-VE, #493-MV), PBS, or 10 μM ISO. For conditioned media treatments, mouse MC3T3 osteoblasts were treated with PBS or 10 μM ISO for 24 hours in 10% FBS αMEM. Media was collected, and a total 500 μL of media were added in the wells. For blocking experiments, mcr84 or a control IgG antibody was added at 100 μg/mL to conditioned media. The experiments were run at 37°C for 12hrs, and pictures were taken under 4× and 10× objectives on an Olympus CKX41 Microscope. Total tube length was analyzed using MetaMorph software. Measurements were performed blinded from treatment/genotype by three persons.

Mouse Vegf ELISA

An ELISA for mouse Vegf was run per manufacturer's instructions (R&D Systems, #MMV00). Media used for this assay was collected from primary BMSCs after 24 hours of either PBS or 10 μM ISO treatment.

Quantitative PCR

Mouse tissues were snap frozen in liquid nitrogen immediately following mouse sacrifice and stored at −80°C. Tissue samples were pulverized with liquid nitrogen-cold mortar and pestle into powder. RNA extraction for both tissues and cells was performed using TRIzol (Life Technologies #15596018). cDNA for qRT-PCR experiments was synthesized using the High Capacity cDNA Reverse Transcription Kit from ABI Applied Biosystems (#1502205). Taqman probes were used to amplify the following genes: Murine *Vegf-a* (Mm00437304), Murine *Hprt* (Mm01545399), Murine *18s (*4333760T), Human *VEGFA* (Hs00900055), and Human *HPRT* (Hs02800695) (6,8). Expression was analyzed by the ΔΔCt method.

Statistics

All data are presented as means ± the standard error mean (SEM). For experiments comparing two groups, a standard two-tailed student's *t* test was used unless otherwise stated in the figure legend. For experiments comparing more than 2 groups, one-way ANOVA was used with a Newman-Keuls post-hoc test unless specifically stated in the figure legend. For all tests, a *p value* less than or equal to .05 was considered significant.

Results

βAR stimulation increases blood vessel formation in post-natal mouse bones

During our previous studies, we noticed the presence of a high number of vascular structures in hind limb sections of mice subjected to daily βAR stimulation by ISO, in which erythrocytes were stained bright red by H&E (6). Because such treatment and chronic stress have been linked to vascular changes in normal physiology and cancer (27–30), we asked whether an increase in sympathetic outflow, typically caused by chronic stress, could alter the vasculature of the adult skeleton and contribute to the efficiency of cancer cells colonization into the skeleton.

To address this question, we reanalyzed the hind limbs of 6 week-old nude mice subjected to a chronic immobilization stress (CIS) protocol (6, 8) that was aimed at stimulating an endogenous stress response. We also analyzed the hind limbs of 6 week-old nude mice treated for 6 weeks daily with the non-selective β1/β2AR agonist isoproterenol (ISO, 3mg/kg ip), used to mimic an increase in sympathetic outflow without stimulating the HPA axis or raising glucocorticoids levels. At endpoint in both models, we measured a 25 to 50% higher vessel area and vessel number per bone marrow area in the treated groups (ISO or CIS) compared to the control groups (Fig. 1A, B).

We then used an *ex vivo* tube formation assay to further define the angiogenic properties associated with ISO treatment and the relevant mode of action. In this experiment, HUVECs as well as CD31-positive, tube-forming primary mouse bone marrow endothelial cells

(BMECs) prepared from WT mice (26) were seeded on growth factor-reduced matrigel in 0% serum endothelial cell growth medium, and treated with PBS or ISO (10μM). Direct treatment of these endothelial cell cultures with ISO did not significantly increase tube length, suggesting that ISO acts indirectly to stimulate bone vessel formation *in vivo* (Supplemental Fig. S1A–C). Therefore, to address the contribution of a putative bone-derived factor to the increase in bone vascular density in response to βAR stimulation, the 24hr-conditioned medium (CM) from PBS or ISO-treated mouse MC3T3 osteoblasts was compared in two independent angiogenesis assays. We first treated HUVEC and BMEC cultures with the CM from PBS or ISO-treated mouse MC3T3 osteoblasts. In both endothelial cell cultures, the CM from ISO-treated osteoblasts increased tube length compared to PBS control (Fig. 1C, D), suggesting that osteoblasts secrete pro-angiogenic factor(s) in response to βAR stimulation. We also cultured metatarsal bone explants from 2 day-old mouse pups in the CM from MC3T3 cultures treated by PBS, ISO (10μM), or the natural βAR ligand norepinephrine (NE, 10 μM) (Fig. 1E). Following 2 weeks, outgrowing blood vessels were labeled by CD31 staining, and vessel sprouting was quantified. We observed that the CM from both NE and ISO-treated osteoblasts caused a significant 80% increase in the number of sprouting parental vessels compared to PBS controls, to a level equal or higher to the one induced by recombinant VEGF, a major angiogenic factor used here as positive control (Fig. 1E, F).

βAR stimulation in osteoblasts increases *Vegf-a* expression and bone angiogenesis

VEGF-A is a well-known pro-angiogenic growth factor. Consistent with the observed increase in blood vessel formation in ISO and CIS-treated mice, its expression level in long bones from mice treated with ISO was 50% higher than in bones from PBS control mice (Fig. 2A).

Multiple cell types within the bone microenvironment, including osteoblasts, express the β2AR and could be the source of the increased *Vegf-a* levels measured in bone following ISO treatment (31). To determine if the osteoblast lineage was one of the principal sources of bone *Vegf-a* secreted in response to βAR agonists, a series of *in vitro* and *in vivo* experiments were performed. First, MC3T3 osteoblast cultures, which represent a pure culture of osteoblastic cells, as well as adherent primary mouse bone marrow stromal cells (BMSCs), were treated with PBS or ISO (10μM). After 2hrs of ISO treatment, *Vegf-a* expression increased 10-fold in MC3T3 cells, and returned to normal levels within 24 hours (Fig. 2B). Similar results were observed with BMSCs treated with ISO, although the response was of lesser intensity, which most likely reflects the more heterogeneous nature of this type of culture (Fig. 2C). *Vegf-a* expression was not increased in ISO-treated BMSCs prepared from β2AR-deficient mice, indicating that in osteoblasts, the β2AR specifically controls *Vegf-a* expression (Fig. 2D). The increase in *Vegf-a* mRNA expression in BMSCs was associated with a 3-fold increase in VEGF protein expression, measured by ELISA (Fig. 2E). Expression of additional angiogenic genes, including other *Vegf* isoforms, *Vegfr2, Ang-2, Fgf2*, and *Pdgfa* in BMSCs was not affected by ISO treatment (Supplemental Fig. S2A–H).

To determine whether osteoblasts are the source of the increased *Vegf-a* expression in response to ISO treatment *in vivo* and whether the β2AR mediates this effect, ISO (3mg/kg) or PBS (control) were administered to mice lacking the β2AR in type I collagen-expressing osteoblasts (*Adrβ2*$^{flox/flox}$; *mouse 2.3kb Col1-cre*, called herein β2AR$_{ob}$KO) or WT mice (*Adrβ2*$^{flox/flox}$, called herein WT) for 6 weeks. At endpoint, femoral vessel density was quantified by measuring the number of endomucin-positive vessels. β2AR$_{ob}$KO mice showed a blunted response to ISO treatment compared to WT mice, as measured by a significant reduction in the number of endomucin-positive vessels compared to ISO-treated WT mice (Fig. 3A–C), and this phenotype was accompanied by a reduction in the number of Vegf-positive osteoblasts per bone surface (Supplemental Fig. S3A, B). Similar results were obtained with mice globally deficient for the β2AR (Supplemental Figs. S4A, B).

Osteoblast-derived VEGF-A promotes bone angiogenesis in response to β2AR stimulation

To confirm that the pro-angiogenic effect induced by β2AR stimulation in osteoblasts was mediated by VEGF-A, we used an antibody (mcr84) that specifically perturbs VEGF-A:VEGFR2 signaling (32–34) in a tube formation assay with BMECs. Upon addition of mcr84 (100μg/mL), the pro-angiogenic effect of the CM from ISO-treated BMSC cultures was significantly attenuated compared to addition of a non-immune IgG. Total tube area and tube length were reduced, and the complexity of the vascular network (average branching points) was lost upon treatment with mcr84 in the presence of CM from ISO-treated osteoblasts (Fig. 4A–D).

The VEGF-A:VEGFR2 blocking properties of mcr84 were then tested *in vivo* to determine if the observed increase in bone blood vessel formation upon β2AR stimulation was mediated by an increase in *Vegf-a* expression. For that purpose, WT C57BL/6 female mice were injected for 6 weeks with either PBS or 3mg/kg ISO daily, along with mcr84 (200 μgs/inj.) or a control IgG antibody twice per week (19). Quantitative analysis of femoral bone sections via immunofluorescence confirmed a 70% increase in endomucin-positive vessel area in the ISO group versus PBS group, and a significant reduction in endomucin-positive vessel area and number in the ISO, mcr84 group compared to the ISO, IgG group (Fig. 5A–C). ISO increased osteoclast number per bone perimeter, as expected from our previous studies, but this osteoclastogenic effect was not affected by mcr84 treatment, suggesting that VEGF-A is not involved in the osteoclastogenic effect of ISO (Supplemental Fig. S5).

The increase in bone vascular density caused by osteoblastic βAR stimulation promotes the colonization of breast cancer cells in bone

Since blood vessels act as conduits through which disseminating tumor cells travel to distant organs, we posited that the stimulatory effects of ISO on osteoblasts, VEGF-A expression, and bone vascular density could contribute to the successful establishment of circulating metastatic cells into the skeleton. This question was addressed experimentally by measuring the bone homing efficiency of bone metastatic triple negative MDA-MB-231 breast cancer cells in response to ISO treatment, in absence of either the β2AR in osteoblasts or VEGF-A:VEGFR2 interaction.

Four week-old female Rag/β2AR$_{ob}$KO or control littermates, Rag/WT, were given PBS or ISO (3mg/kg) ip injections for 3 weeks, a dosing and time frame verified to allow a significant increase in long bone blood vessel density (Supplemental Fig. S6). The day following the last injection, 10^5 osteotropic MDA-MB-231 breast cancer cells were inoculated into the left cardiac ventricle. We used this model of cancer cell inoculation to specifically focus on the late phase of the metastatic process, excluding confounding factors related to a possible effect of ISO on the primary tumor. The skeletal colonization of metastatic MDA-MB-231 cells was assessed 4 weeks later by radiographic and histological analyses. Confirming our previous results in nude mice (6), we observed that the area and number of long bone metastatic osteolytic lesions on X-rays was more than 50% higher in ISO-treated WT mice compared to PBS-treated WT mice (Fig. 6A–C). Importantly, lack of the β2AR in Rag/β2AR$_{ob}$KO mice blunted the stimulatory effect of ISO on bone lesion area and number. X-rays lesions were verified by the presence of cancer cells at sites of lesion by histology (Fig. 6D).

In a second experiment, four week-old *Rag2*/WT mice were treated with PBS or ISO as above for 3 weeks, in combination with the VEGF-blocking antibody, mcr84 (200 μgs/inj., twice per week), or a control IgG2 antibody. The day following the last injection, 10^5 osteotropic MDA-MB-231 breast cancer cells were inoculated via the intracardiac route, and mice were sacrificed 4 weeks later. Radiographic and histological analyses again confirmed an increase in bone colonization upon ISO treatment (Fig. 7A–D), and similarly to the lack of β2AR, mcr84 treatment significantly reduced the number and area of bone lesions compared to ISO and IgG-treated mice. Confirming our previous results, we found that average total bone tumor area was increased in ISO-treated mice, but the average area of each bone tumor foci was unchanged, suggesting that the action of ISO on the bone microenvironment mainly affects the colonization efficiency of metastatic cancer cells, and not their growth in bone (Supplemental Fig. S7). Together with the β2AR-dependent increase in bone blood vessel number induced by ISO treatment shown above, these results support a model in which increased sympathetic outflow in mice triggers a VEGF-dependent neo-angiogenic switch in the bone microenvironment, via stimulation of the β2AR in osteoblasts, favoring the early skeletal establishment of metastatic cancer cells.

Discussion

The vasculature is essential for tumor growth and escape of metastatic cells from the primary tumor, and pro-angiogenic pathways became and still are a major target of many cancer therapeutic drugs (4–5, 19, 32–38). We show here that an increase in vascular density can be induced in the mouse bone microenvironment following stimulation of the β2AR by ISO treatment, which mimics a state of high sympathetic outflow. Through *in vitro* and *in vivo* loss-of-function approaches, we show that these changes in bone vascular density are mediated in part by an increase in Vegf-a expression and the β2AR expressed in osteoblasts. We also provide experimental evidence that this increase in bone vascular density favors the skeletal colonization efficiency of bone metastatic MDA-MB-231 cells. Together, these results strengthen the importance of sympathetic nerves and chronic SNS activation in the process of metastatic bone colonization, and implicate neo-angiogenesis in this process.

The effect of stress on sympathetic nerve activity has beneficial consequences in the short term (fight-or-flight response), but can lead to a wide range of pathologies if it becomes chronic, as the SNS regulates the homeostasis of many peripheral organs (27). We have previously shown that bone remodeling and the expression of RANKL by osteoblasts are under the control of sympathetic nerves (6,14). RANKL is well known for its osteoclastogenic properties, and its pro-migratory effects on metastatic cancer cells have been more recently demonstrated (39–41). In the specific context of breast cancer, we have shown that ISO treatment leads to increased number of bone metastatic tumors following intracardiac injection of MDA-MB-231 breast cancer cells (6). An increase in the size of osteolytic lesions in these conditions was expected as ISO treatment increases RANKL, osteoclastogenesis, and bone resorption, thus feeding the osteolytic bone destruction associated with the presence of breast cancer cells in bone (42). However, the observed increase in the number of metastatic foci and bone osteolytic lesions suggested a specific effect on cancer cell colonization. This was demonstrated in this model by restricting ISO treatment prior to cancer cell inoculation, in order to affect the bone microenvironment without directly impacting the behavior of metastatic cancer cells. In this experiment, bone colonization by cancer cells was still increased, confirming a major effect of ISO on the bone microenvironment, and likely via osteoblasts. Additional *in vitro* and *in vivo* experiments demonstrated the contribution of RANKL to the bone homing response observed in these conditions that mimic chronic SNS activation (6). Our new findings related to the effect of ISO on bone vascularity thus suggest that the activity of sympathetic nerves in the bone microenvironment can influence the pre-metastatic niche via at least two mechanisms: 1) by increasing the likelihood of bone colonization through a higher density of blood vessels, and 2) by promoting the migration of breast cancer cells after extravasation into the bone marrow toward the RANKL-secreting osteoblastic niche. Of note, the effect of increased sympathetic outflow on vascular structures in the context of metastasis is not limited to the bone microenvironment, as chronic stress also promotes breast cancer cell intravasation into lymphatic vessels in mice, via a Vegf-c:Cox-2 mechanism (43). In addition, the increased number of tumor-induced bone lesions in ISO-pretreated mice was interpreted to reflect more efficient tumor cell colonization of the skeleton, but one cannot exclude an effect on blood and nutrient supply leading to increased tumor growth after cells have reached the bone microenvironment, even if initial tumor bone colonization was equivalent in control and ISO-treated groups. However, the observation that the average size of single bone tumors per mouse was not significantly different between groups does not support the latter mechanism.

It has been shown that multiple tumor types express adrenergic receptors and benefit from their activation in term of growth or survival (44–46). Our experimental set up of a 3-week ISO pre-treatment, prior to MDA-MB-231 inoculation, however exposes tumor cells to negligible levels of ISO, thus supporting the key role of the stroma in the higher bone colonization efficiency observed following β2AR stimulation. The fact that ablation of the β2AR in osteoblasts blunted the average number of Vegf-a-positive osteoblasts and the increase in blood vessel density following ISO treatment brings further evidence that the osteoblast is one of the main cell responsive to sympathetic nerves in bone.

The molecular mechanism whereby β2AR stimulation in osteoblasts leads to increased Vegf-a expression remains to be identified. The contribution of HIF-1α or HIF-2α to a β2AR-dependent increase in VEGF-A expression needs to be addressed, as expression of HIF-1α or HIF-2α can be controlled in a hypoxia-independent manner (47, 48). In addition, the bone vasculature is composed of different types of endothelial cells that respond to different signaling pathways (49, 50). Which specific population of endothelial cells is involved in the ISO-induced neo-angiogenesis reported here needs to be further defined. Lastly, it can be noticed that the inhibitory effect of Vegf-a blockade on ISO-induced angiogenesis was partial. Although a suboptimal dose or treatment regimen could explain this observation, it cannot be excluded that other angiogenic factors than Vegf, Fgf2, Angpt2 and Pdgfa are involved.

From a therapeutic point of view, angiogenesis, being a normal physiological process, imposes limitations and difficulties as a therapeutic target for cancer treatments. This partially explains why the clinical use of VEGF inhibitors, although beneficial in certain cancers, is still limited by adverse effects, toxicity, and acquired drug resistance (51). Contrastingly, the use of β-blockers as adjuvant therapy in patients diagnosed with breast cancer may have several therapeutic advantages. If both Vegf-a and Rankl are β2AR target genes and critical mediators of bone resorption, angiogenesis and metastatic cancer cell colonization of bone, the use of a single drug with β-blockade activity has the potential of reducing bone resorption, angiogenesis, and bone tumor establishment in at-risk patients (52). These properties could make β-blockers particularly efficacious in preventing disseminated cancer cells from reaching the safe heaven of the bone microenvironment and may expose these cells more readily to chemotherapy or actions of the immune system. In that regard, several preclinical and clinical studies have shown a benefit from β-blocker use on survival in patients with triple negative breast cancer, non-small cell lung cancer, hemangiomas, and ovarian cancer (10, 12, 20, 29–30, 53–55). Whether this protective effect is mediated through a reduction in cancer cell growth, bone metastasis, or other mechanism(s) remains unknown.

In conclusion, this work supports the importance of sympathetic nerve activation on breast cancer bone colonization and identifies an osteoblastic, β2AR- and VEGF-A-dependent neo-angiogenic switch mechanism contributing to this effect. It provides suggestive preclinical evidence in mice that targeted therapies that prevent these vascular changes could improve treatment outcomes for women diagnosed with breast cancer; especially for women subjected to chronic stress, such as those with poor socioeconomic status or facing challenging familial situations. These preclinical findings need to be further investigated clinically.

Supplementary Material

Refer to Web version on PubMed Central for supplementary material.

Acknowledgments

The authors thank Lejla Pasic for her help with the confocal microscopy experiments, and Drs. J. Penn, G. Holt and J. Chen for their valuable comments.

Grant Supporters: This work was supported by the following grants: NCI (R01CA 168 717 to FE, R01 CA163 199 to JAS, F31 CA192 748 to PLM), and The Department of Veteran's Affairs (1 I01 BX 001 957 to JAS).

References

1. American Cancer Society. Cancer Facts & Figures. Vol. 2016. Atlanta: American Cancer Society; 2016.
2. Costa L, Badia X, Chow E, Lipton A, Wardley A. Impact of skeletal complications on patients' quality of life, mobility, and functional independence. Support Care Cancer [Internet]. 2008 Aug; 16(8):5. 879–89.
3. Hassan S, Karpova Y, Baiz D, Yancey D, Pullikuth A, Flores A, Register T, Cline JM, D'Agostino R, Danial N, Datta SR, Kulik G. Behavioral stress accelerates prostate cancer development in mice. J Clin Invest. 2013 Feb; 123(2):5. 874–86.
4. Pratt LA, Brody DJ. Depression in the US Household Population. 2009–2012NCHS Data Brief. No. 172,2014
5. Palesh O, Butler LD, Koopman C, Giese-Davis J, Carlson R, Spiegel D. Stress History and Breast Cancer Recurrence. Journal of psychosomatic research. 2007; 63(3):233–239. [PubMed: 17719359]
6. Campbell JP, Karolak MR, Ma Y, Perrien DS, Masood-Campbell SK, Penner L, Munoz SA, Zijlstra A, Yang X, Sterling JA, Elefteriou F. Stimulation of host bone marrow stromal cells by sympathetic nerves promotes breast cancer bone metastasis in mice. PLoS Biol. 2012 Jul.10(7)
7. Campbell JP, Merkel AR, Masood-Campbell SK, Elefteriou F, Sterling JA. Models of Bone Metastasis. J Vis Exp. 2012; (67):e4260. [PubMed: 22972196]
8. Preston Campbell J, Mulcrone P, Masood SK, Karolak M, Merkel A, Hebron K, Zijlstra A, Sterling J, Elefteriou F. TRIzol and Alu qPCR-based quantification of metastatic seeding within the skeleton. Sci Rep. 2015 Jan.5:4. 12635.
9. Chida Y, Hamer M, Wardle J, Steptoe A. Do stress-related psychosocial factors contribute to cancer incidence and survival? . Nat Clin Pract Oncol. 2008 Aug; 5(8):5. 466–75.
10. Melhem-Bertrandt A, Chavez-Macgregor M, Lei X, Brown E, Lee R, Meric-Bernstam F, Sood A, Conzen S, Hortobagyi G, Gonzalez-Angulo A-M. Beta-blocker use is associated with improved relapse-free survival in patients with triple-negative breast cancer. Journal of Clinical Oncology: official journal of the American Society of Clinical Oncology. 2011; 29(19):2645–52. [PubMed: 21632501]
11. Hill EL, Elde R. Distribution of CGRP-, VIP-, D H-, SP-, and NPY-immunoreactive nerves in the periosteum of the rat. Cell and tissue research [Internet] Springer. 1991; 264(3):469–80.
12. Thaker PH, Han LY, Kamat AA, Arevalo JM, Takahashi R, Lu C, Jennings NB, Armaiz-Pena G, Bankson JA, Ravoori M, Merritt WM, Lin YG, Mangala LS, Kim TJ, Coleman RL, Landen CN, Li Y, Felix E, Sanguino AM, Newman RA, Lloyd M, Gershenson DM, Kundra V, Lopez-Berestein G, Lutgendorf SK, Cole SW, Sood AK. Chronic stress promotes tumor growth and angiogenesis in a mouse model of ovarian carcinoma. Nat Med [Internet]. 2006 Aug; 12(8):2. 939–44.
13. Takeda S, Elefteriou F, Levasseur R, Liu X, Zhao L, Parker KL, Armstrong D, Ducy P, Karsenty G. Leptin regulates bone formation via the sympathetic nervous system. Cell. 2002 Nov; 111(3):5. 305–17. [PubMed: 12372294]
14. Asada N, Katayama Y, Sato M, Minagawa K, Wakahashi K, Kawano H, Kawano Y, Sada A, Ikeda K, Matsui T, Tanimoto M. Matrix-embedded osteocytes regulate mobilization of hematopoietic stem/progenitor cells. Cell Stem Cell. 2013 Jun; 12(6):4. 737–47.
15. Itoh Y, Yamada M, Suematsu N, Matsushita M, Otomo E. An immunohistochemical study of centenarian brains: a comparison. J Neurol Sci. 1998 Apr; 157(1):3. 73–81.
16. Yasuda H, Shima N, Nakagawa N, Yamaguchi K, Kinosaki M, Mochizuki S, Tomoyasu A, Yano K, Goto M, Murakami A, Tsuda E, Morinaga T, Higashio K, Udagawa N, Takahashi N, Suda T. Osteoclast differentiation factor is a ligand for osteoprotegerin/osteoclastogenesis-inhibitory factor and is identical to TRANCE/RANKL. Proc Natl Acad Sci USA. 1998 Mar; 95(7):2. 3597–602. [PubMed: 9419315]

17. Sloan EK, Priceman SJ, Cox BF, Yu S, Pimentel MA, Tangkanangnukul V, Arevalo JM, Morizono K, Karanikolas BD, Wu L, Sood AK, Cole SW. The sympathetic nervous system induces a metastatic switch in primary breast cancer. Cancer Res [Internet]. 2010 Sep; 70(18):3. 7042–52.

18. Santini D, Perrone G, Roato I, Godio L, Pantano F, Grasso D, Russo A, Vincenzi B, Fratto ME, Sabbatini R, Della Pepa C, Porta C, Del Conte A, Schiavon G, Berruti A, Tomasino RM, Papotti M, Papapietro N, Onetti Muda A, Denaro V, Tonini G. Expression pattern of receptor activator of NFκB (RANK) in a series of primary solid tumors and related bone metastases. J Cell Physiol [Internet]. 2011 Mar; 226(3):2. 780–4.

19. Sullivan LA, Carbon JG, Roland CL, Toombs JE, Nyquist-Andersen M, Kavlie A, Schlunegger K, Richardson JA, Brekken RA. R84, a novel therapeutic antibody against mouse and human VEGF with potent anti-tumor activity and limited toxicity induction. PloS ONE. 2010 Jan 5.5(8):e12031. [PubMed: 20700512]

20. Roland CL, Dineen SP, Lynn KD, Sullivan LA, Dellinger MT, Sadegh L, Sullivan JP, Shames DS, Brekken RA. Inhibition of vascular endothelial growth factor reduces angiogenesis and modulates immune cell infiltration of orthotopic breast cancer xenografts. Mol Cancer Ther. 2009 Jul; 8(7):3. 1761–71.

21. Dacquin R, Starbuck M, Schinke T. Mouse α1 (I)-collagen promoter is the best known promoter to drive efficient Cre recombinase expression in osteoblast. Developmental … [Internet]. 2002

22. Kajimura D, Hinoi E, Ferron M, Kode A, Riley KJ, Zhou B, Guo XE, Karsenty G. Genetic determination of the cellular basis of the sympathetic regulation of bone mass accrual. J Exp Med. 2011 Apr; 208(4):1. 841–51.

23. Yoneda T, Williams PJ, Hiraga T, Niewolna M, Nishimura R. A Bone-Seeking Clone Exhibits Different Biological Properties from the MDA-MB-231 Parental Human Breast Cancer Cells and a Brain-Seeking Clone In Vivo and In Vitro. JBMR. 2001; 16

24. Pasic L, Eisinger-Mathason T, Velayudhan B, Moskaluk C, Brenin D, Macara I, Lannigan D. Sustained activation of the HER1-ERK1/2-RSK signaling pathway controls myoepithelial cell fate in human mammary tissue. Gene Dev. 2011; 25(15):1641–53. [PubMed: 21828273]

25. Deckers MM, Smits P, Karperien M, Ni J, Tylzanowski P, Feng P, Parmelee D, Zhang J, Bouffard E, Gentz R, Löwik CW, Merregaert J. Recombinant human extracellular matrix protein 1 inhibits alkaline phosphatase activity and mineralization of mouse embryonic metatarsals in vitro. Bone. 2001 Jan; 28(1):1. 14–20. [PubMed: 11165936]

26. Sekiguchi H, Ii M, Jujo K, Yokoyama A, Hagiwara N, Asahara T. Improved culture-based isolation of differentiating endothelial progenitor cells from mouse bone marrow mononuclear cells. PloS ONE. 2011 Jan 6.6(12):e28639. [PubMed: 22216102]

27. Golbidi S, Frisbee JC, Laher I. Chronic stress impacts the cardiovascular system: animal models and clinical outcomes. Am J Physiol Heart Circ Physiol. 2015 Jun; 308(12):1. H1476–98.

28. Madden KS, Szpunar MJ, Brown EB. B-Adrenergic receptors (β-AR) regulate VEGF and IL-6 production by divergent pathways in high β-AR-expressing breast cancer cell lines. Breast Cancer Res Treat [Internet]. 2011 Dec; 130(3):4. 747–58.

29. Chen, Ji Y., Li, S., Xiao, K., Zheng, X., Xu, ST. The role of β-adrenergic receptor signaling in the proliferation of hemangioma-derived endothelial cells. Cell Div [Internet]. 2013 Jan.8(1):2. 1.

30. Stiles JM, Amaya C, Rains S, Diaz D, Pham R, Battiste J, Modiano JF, Kokta V, Boucheron LE, Mitchell DC, Bryan BA. Targeting of beta adrenergic receptors results in therapeutic efficacy against models of hemangioendothelioma and angiosarcoma. PloS ONE [Internet]. 2013; 8:e60021.

31. Ma Y, Nyman JS, Tao H, Moss HH, Yang X, Elefteriou F. β2-Adrenergic receptor signaling in osteoblasts contributes to the catabolic effect of glucocorticoids on bone. Endocrinology. 2011 Apr; 152(4):5. 1412–22.

32. Roland CL, Lynn KD, Toombs JE, Dineen SP, Udugamasooriya DG, Brekken RA. Cytokine levels correlate with immune cell infiltration after anti-VEGF therapy in preclinical mouse models of breast cancer. PloS ONE. 2009; 4

33. Sullivan LA, Brekken RA. The VEGF family in cancer and antibody-based strategies for their inhibition. MAbs. 2010 Jan; 2(2):5. 165–75.

34. Yang L, Kwon J, Popov Y, Gajdos GB, Ordog T, Brekken RA, Mukhopadhyay D, Schuppan D, Bi Y, Simonetto D, Shah VH. Vascular endothelial growth factor promotes fibrosis resolution and repair in mice. Gastroenterology. 2014 May; 146(5):4. 1339–50.e1.
35. Yu, Gu X., Dai, XH. Intravitreal injection of ranibizumab for treatment of age-related macular degeneration: effects on serum VEGF concentration. Curr Eye Res. 2014 May; 39(5):4. 518–21.
36. Yu L, Wu X, Cheng Z, Lee CV, LeCouter J, Campa C, Fuh G, Lowman H, Ferrara N. Interaction between bevacizumab and murine VEGF-A: a reassessment. Invest Ophthalmol Vis Sci. 2008 Feb; 49(2):5. 522–7.
37. Gao D, Nolan DJ, Mellick AS, Bambino K, McDonnell K, Mittal V. Endothelial progenitor cells control the angiogenic switch in mouse lung metastasis. Science [Internet]. 2008 Jan; 319(5860):5. 195–8.
38. Song F-N, Duan M, Liu L-Z, Wang Z-C, Shi J-Y, Yang L-X, et al. RANKL Promotes Migration and Invasion of Hepatocellular Carcinoma Cells via NF-κB-Mediated Epithelial-Mesenchymal Transition. PLoS ONE. 2014; 9(9)
39. Armstrong AP, Miller RE, Jones JC, Zhang J, Keller ET, Dougall WC. RANKL acts directly on RANK-expressing prostate tumor cells and mediates migration and expression of tumor metastasis genes. Prostate. 2008 Jan; 68(1):2. 92–104.
40. Cheng ML, Fong L. Effects of RANKL-Targeted Therapy in Immunity and Cancer. Front Oncol. 2014 Jan.3:2. 329.
41. Mundy GR. Metastasis to Bone: Causes, Consequences, and Therapeutic Opportunities. Nat Rev Cancer. 2002 Aug; 2(8):4. 584–93.
42. Le CP, Nowell CJ, Kim-Fuchs C, Botteri E, Hiller JG, Ismail H, Pimentel MA, Chai MG, Karnezis T, Rotmensz N, Renne G, Gandini S, Pouton CW, Ferrari D, Möller A, Stacker SA, Sloan EK. Chronic stress in mice remodels lymph vasculature to promote tumour cell dissemination. Nat Commun. 2016 Jan.7:5. 10634.
43. Creed SJ, Le CP, Hassan M, Pon CK, Albold S, Chan KT, Berginski ME, Huang Z, Bear JE, Lane JR, Halls ML, Ferrari D, Nowell CJ, Sloan EK. β2-adrenoceptor signaling regulates invadopodia formation to enhance tumor cell invasion. Breast Cancer Res. 2015 Nov.17(1):3. 145. [PubMed: 25572662]
44. Nagaraja AS, Dorniak PL, Sadaoui NC, Kang Y, Lin T, Armaiz-Pena G, Wu SY, Rupaimoole R, Allen JK, Gharpure KM, Pradeep S, Zand B, Previs RA, Hansen JM, Ivan C, Rodriguez-Aguayo C, Yang P, Lopez-Berestein G, Lutgendorf SK, Cole SW, Sood AK. Sustained adrenergic signaling leads to increased metastasis in ovarian cancer via increased PGE2 synthesis. Oncogene. 2016 May; 35(18):4. 2390–7.
45. Hulsurkar M, Li Z, Zhang Y, Li X, Zheng D, Li W. Beta-adrenergic signaling promotes tumor angiogenesis and prostate cancer progression through HDAC2-mediated suppression of thrombospondin-1. Oncogene. 2016 Sep.:1.
46. Sastry KS, Karpova Y, Prokopovich S, Smith AJ, Essau B, Gersappe A, Carson JP, Weber MJ, Register TC, Chen YQ, Penn RB, Kulik G. Epinephrine protects cancer cells from apoptosis via activation of cAMP-dependent protein kinase and BAD phosphorylation. J Biol Chem. 2007 May; 282(19):5. 14094–100. [PubMed: 17082179]
47. Saito T, Fukai A, Mabuchi A, Ikeda T, Yano F, Ohba S, Nishida N, Akune T, Yoshimura N, Nakagawa T, Nakamura K, Tokunaga K, Chung U-II, Kawaguchi H. Transcriptional regulation of endochondral ossification by HIF-2alpha during skeletal growth and osteoarthritis development. Nat Med. 2010 Jun; 16(6):2. 678–86.
48. Zelzer E, Levy Y, Kahana C, Shilo BZ, Rubinstein M, Cohen B. Insulin induces transcription of target genes through the hypoxia-inducible factor HIF-1alpha/ARNT. EMBO J. 1998 Sep; 17(17): 2. 5085–94.
49. Kusumbe AP, Ramasamy SK, Adams RH. Coupling of angiogenesis and osteogenesis by a specific vessel subtype in bone. Nature. 2014 Mar; 507(7492):4. 323–8.
50. Ramasamy SK, Kusumbe AP, Wang L, Adams RH. Endothelial Notch activity promotes angiogenesis and osteogenesis in bone. Nature. 2014 Mar; 507(7492):4. 376–80.
51. Dy GK, Adjei AA. Understanding, recognizing, and managing toxicities of targeted anticancer therapies. CA Cancer J Clin. 2013 Jan; 63(4):2. 249–79.

52. Elefteriou F. Chronic stress, sympathetic activation and skeletal metastasis of breast cancer cells. Bonekey Rep. 2015 Jan.4:4. 693.

53. Pasquier E, Ciccolini J, Carre M, Giacometti S, Fanciullino R, et al. Propranolol potentiates the anti-angiogenic effects and anti-tumor efficacy of chemotherapy agents: implication in breast cancer treatment. Oncotarget. 2011; 2:797–809. [PubMed: 22006582]

54. Barron TI, Sharp L, Visvanathan K. Beta-adrenergic blocking drugs in breast cancer: a perspective review. Therapeutic Advances in Medical Oncology. 2012; 4(3):113–125. 2012. [PubMed: 22590485]

55. Wang HM, Liao ZX, Komaki R, Welsh JW, O'Reilly MS, Chang JY, Zhuang Y, Levy LB, Lu C, Gomez DR. Improved survival outcomes with the incidental use of beta-blockers among patients with non-small-cell lung cancer treated with definitive radiation therapy. Ann Oncol [Internet]. 2013; 24:1312–9.

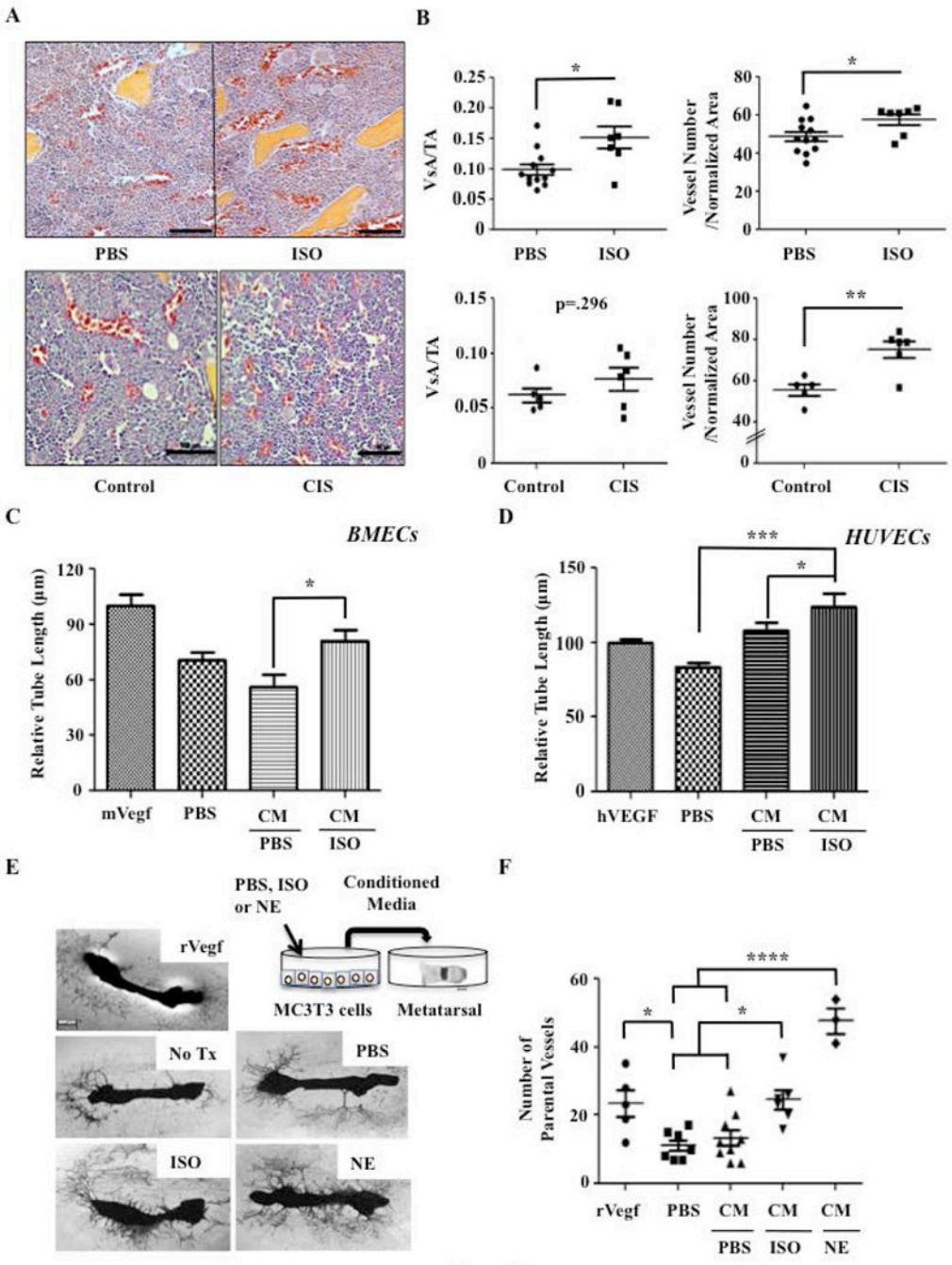

Figure 1. Isoproterenol Treatment Increases Skeletal Blood Vessel density

A) Representative 40× H&E images of hind limb bone sections from athymic nude mice treated with PBS, 3mg/kg Isoproterenol (ISO), or Chronic Immobilization Stress (CIS). Blood vessels can be recognized by their shape and staining of red blood cells (red). Bar: 100 μm. B) Quantification of vessel area (VsA) and vessel number normalized by tissue area (TA) in mice that received PBS (N=12) or ISO (N=7) (p=.009 and p=.037), as well as mice subjected to control (N=5) or CIS (N=6) (p=.296 and p=.004). C) Quantification of primary mouse BMEC tube length (*=p<.05, N=3). D) Quantification of HUVECs tube length

(*p=<.05, ***=p<.001, N=6). E) Schematic of the metatarsal assay and representative 4× Images of metatarsals according to each treatment. After 2 weeks of culture, mouse explants were stained for the endothelial cell marker CD31. F) Quantification of the number of CD31+ parental vessels sprouting from the metatarsal bones (*P=<.05, ****P=<.0001, N≥3).

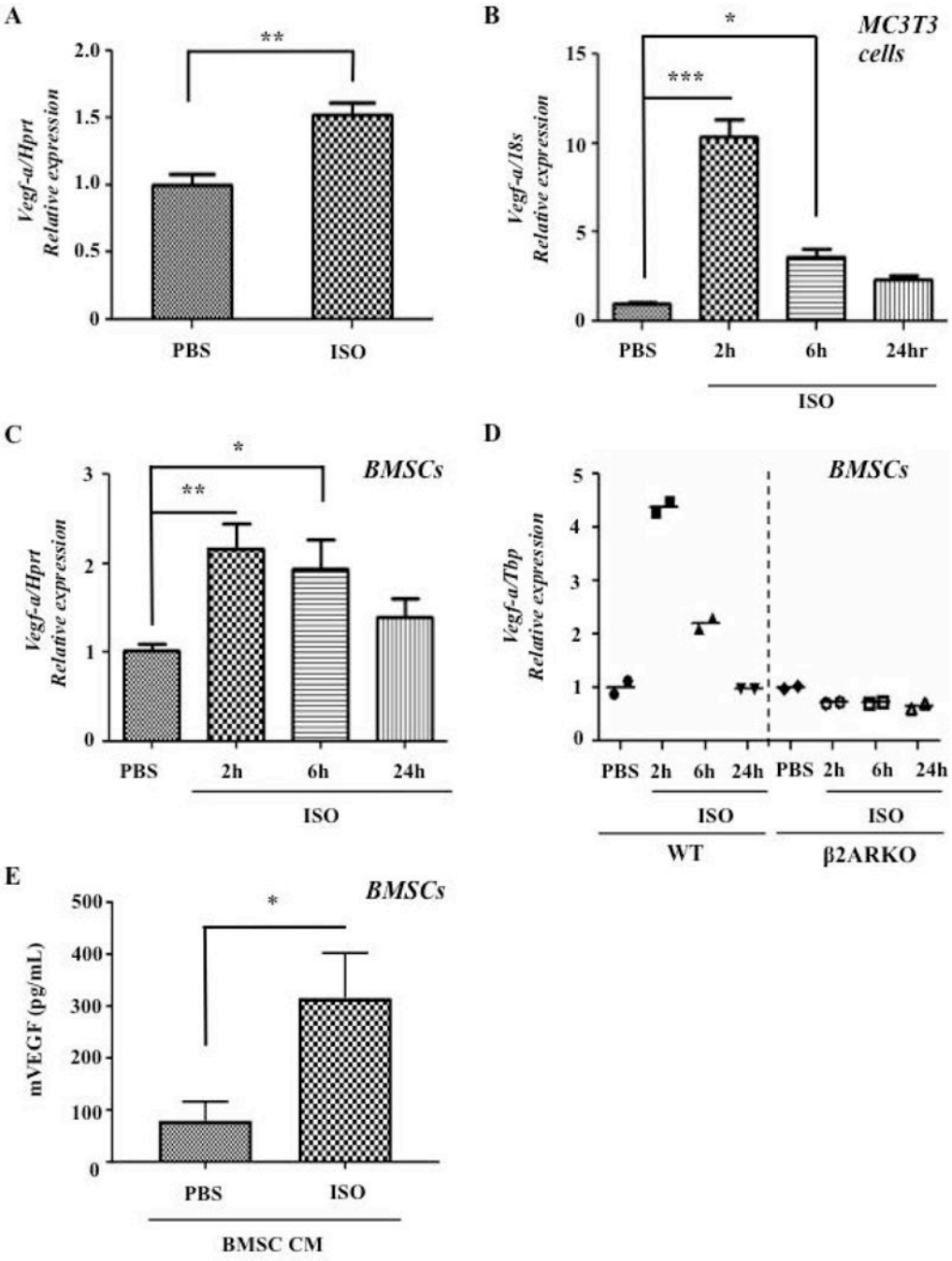

Figure 2. ISO Increases Vegf-a Bone Levels both *In Vivo* and *In Vitro*

A) ISO (2 hrs, 3mg/kg, IP) increases *Vegf-a* expression significantly in whole mouse bone, P=.0064 (qPCR, N=3 for ISO, N=5 for PBS). B) ISO increases expression of *Vegf-a* in MC3T3 mouse osteoblasts, P<.001 (qPCR, N=3). C) ISO increases expression of *Vegf-a* in primary mouse BMSCs, P=.012 (qPCR, N=6). D) *Vegf-a* expression does not increase upon ISO treatment in β2ARKO BMSCs (qPCR, N=2). E) ISO-treated CM from BMSC contains higher amounts of mVegf (N=5, p=.0159 via Mann Whitney U Test, *P=<.05, **P=<.01, ***P=<.001).

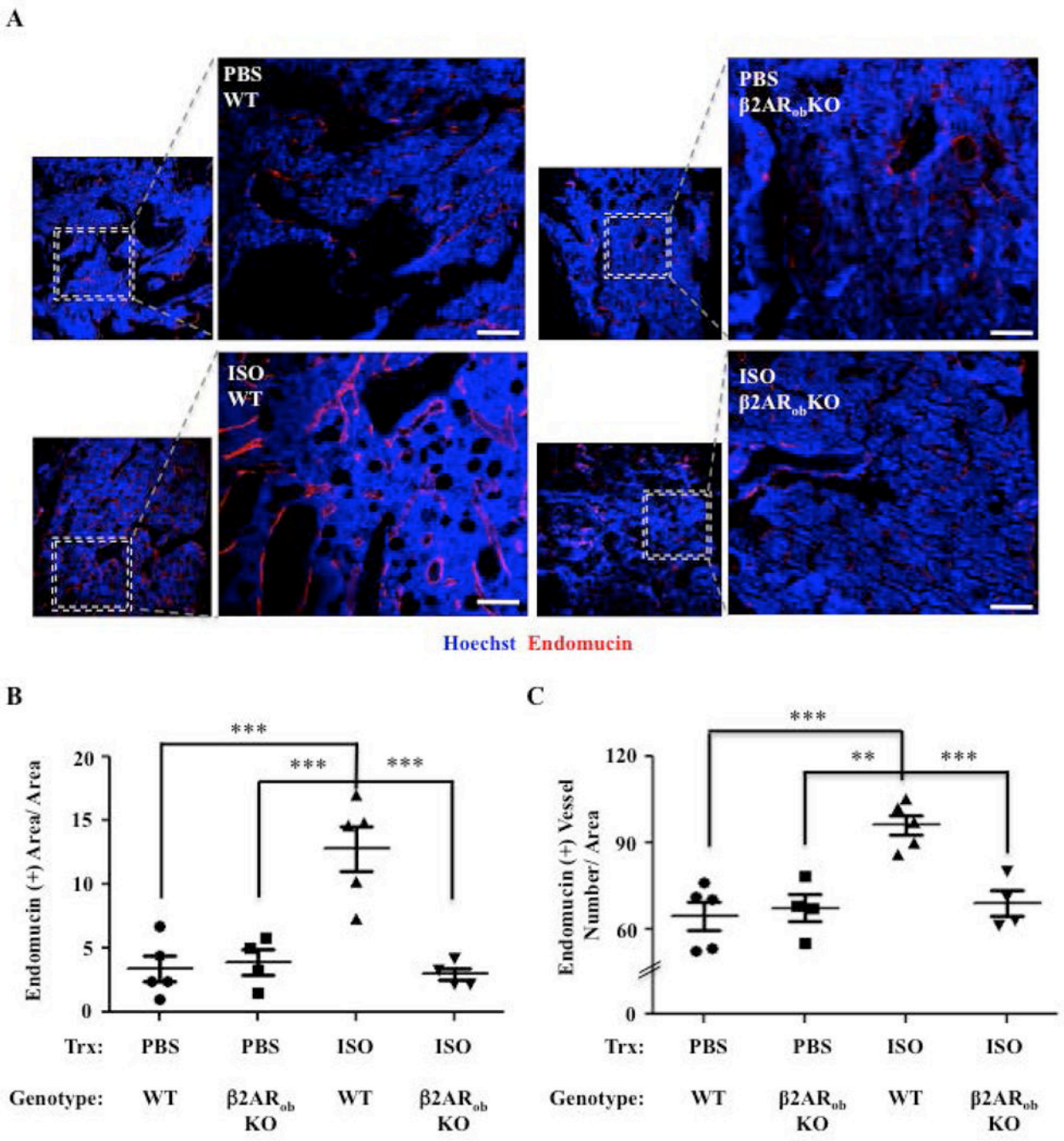

Figure 3. Genetic Loss of β2AR in Osteoblasts Prevents the Increase in Bone Vascular Density Induced by ISO

A) Representative 10× and 20× confocal images of hind limb bone sections from WT and β2AR$_{ob}$KO mice treated with PBS or ISO for 6 weeks, stained for endomucin (IF, red). Bar: 100 μm. Hoechst = Blue. B) Quantification of Endomucin (+) Area/Total Area (N=4–5). C) Quantification of the number of Endomucin (+) Vessels/Area (N=4–5) (*P=<.05, ** P =<.01 *** P =<.001).

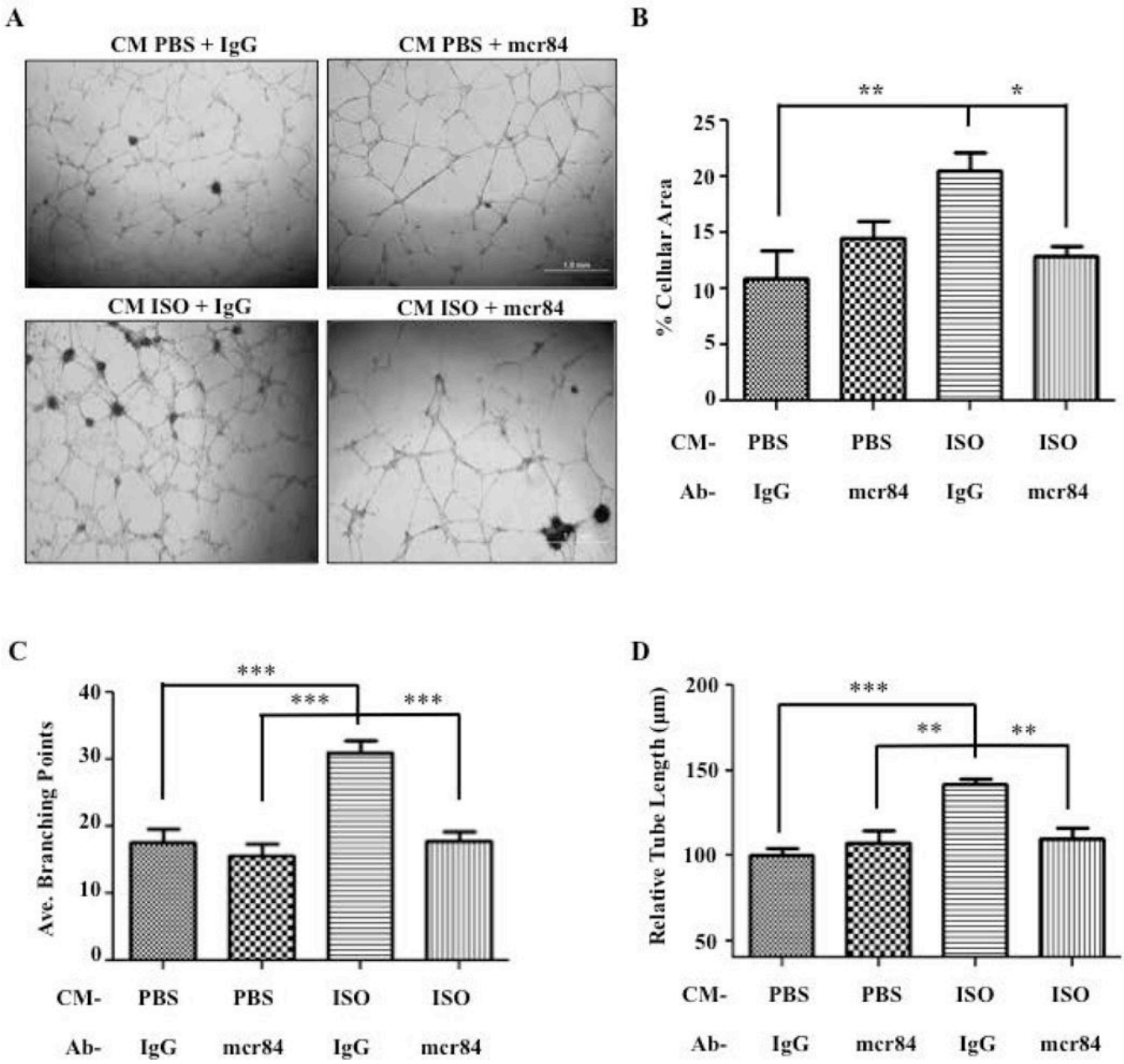

Figure 4. Blocking Vegf-a:Vegfr2 Signaling Diminishes the Effects of the Conditioned Media from ISO-treated BMSCs on Primary Endothelial Tube Formation *in vitro*

A) 4× phase contrast images of mouse BMECs differentiated on Matrigel and receiving the conditioned media from mouse MC3T3 osteoblasts treated with PBS or ISO, and with either mcr84 (100ugs/mL) or IgG2a control antibody for 12 hrs. B) Quantification of the percentage of cellular area used as an assessment of tube formation after 12 hours. (P=.003). C) Average branching points (P<.001). D) Relative tube length was also used to measure tube formation. (P<.001) (**=<.05, **=<.01, ***=<.001*, N=6 for each analysis).

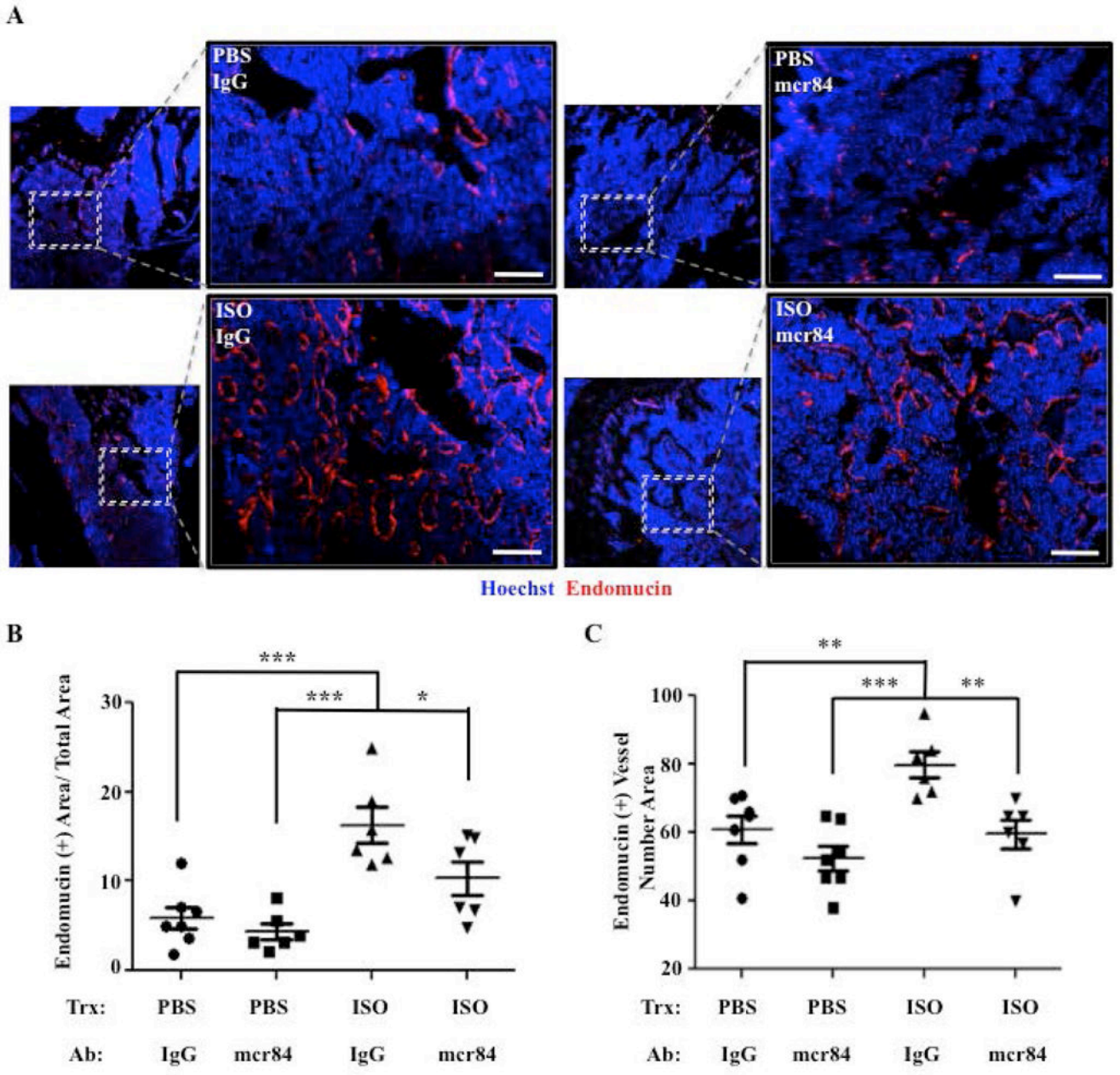

Figure 5. Blocking the Interaction Between Vegf-a and Vegfr2 Reduces the Increase in Bone Vascular Density Caused by ISO Administration

A) Representative 10× and 20× confocal images of hind limb paraffin sections from mice treated with PBS or ISO, and with either mcr84 or IgG2a control antibody for 6 wks, stained for endomucin (IF, red). Hoechst= Blue. Bar: 100 μm. B) Quantification of the Endomucin-positive area/Total Area. C) Quantification of the number of Endomucin (+) Vessels/Area (*P=<.05, **P=<.01, ***P=<.001, N=6–7).

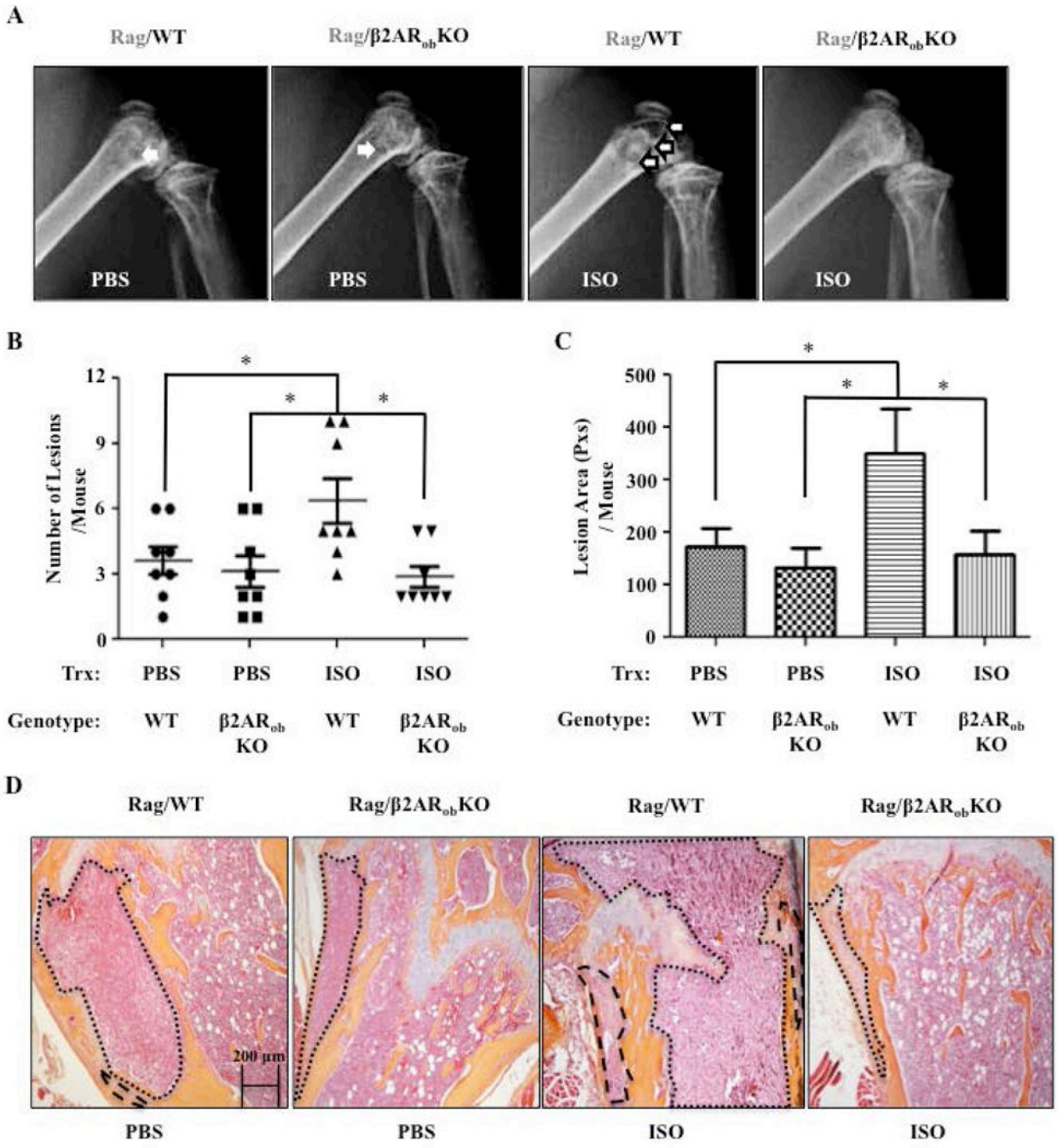

Figure 6. Absence of β2AR in Osteoblasts Limits Tumor Seeding of Bone Caused by ISO Treatment

A) Representative X-rays of hind limbs 28 days following intracardiac inoculation of osteotropic MDA-MB-231 breast cancer cells in Rag/WT and Rag/β2AR$_{ob}$KO mice that received PBS or ISO for 3 weeks, prior to cancer cell inoculation. B) Quantification of lesions in the forelimbs and hind limbs of mice detected by full-body X-ray at day 28 post IC injection (*P=<.05, N=8). C) Average lesion area per mouse, calculated from the same X-ray images (*P=<.05, N=8). D) 20× H&E Images of mouse femurs. Tumors are outlined in black.

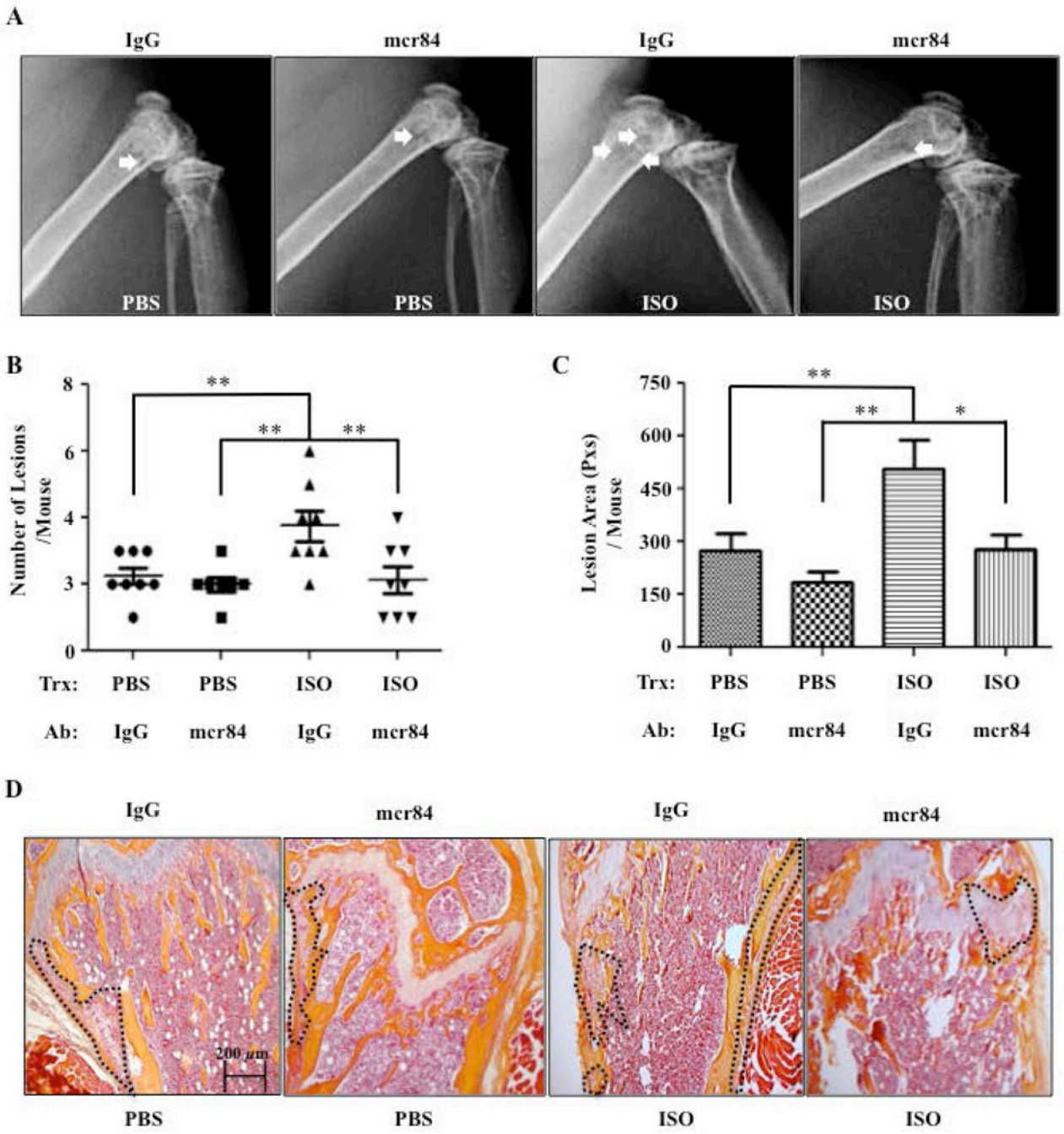

Figure 7. Blocking the Interaction Between Vegf-a and Vegfr2 Prevents the Stimulatory Effect of ISO on Tumor Seeding in Bones

A) Representative X-rays of hind limbs 28 days following intracardiac inoculation of osteotropic MDA-MB-231 breast cancer cells in *Rag2*−/− mice treated with PBS or ISO, and with either mcr84 or an IgG2a control antibody. B) Quantification of lesions in the forelimbs and hind limbs of mice detected by full-body X-ray at day 28 post IC injection (N=7–8). C) Average lesion area per mouse, calculated from the same X-ray images (*P=<.05, **P=<.01, N=7–8). D) 20× H&E Images of mouse femurs. Tumors are outlined in black